
Data augmentation for efficient learning from parametric experts

Alexandre Galashov¹ Josh Merel¹ Nicolas Heess¹

Abstract

We present a simple, yet effective data-augmentation technique to enable data-efficient learning from parametric experts for reinforcement and imitation learning. We focus on what we call the *policy cloning* setting, in which we use online or offline queries of an expert or expert policy to inform the behavior of a student policy. This setting arises naturally in a number of problems, for instance as variants of behavior cloning, or as a component of other algorithms such as DAGGER, policy distillation or KL-regularized RL. Our approach, *augmented policy cloning* (APC), uses synthetic states to induce feedback-sensitivity in a region around sampled trajectories, thus dramatically reducing the environment interactions required for successful cloning of the expert. We achieve highly data-efficient transfer of behavior from an expert to a student policy for high-degrees-of-freedom control problems. We demonstrate the benefit of our method in the context of several existing and widely used algorithms that include policy cloning as a constituent part. Moreover, we highlight the benefits of our approach in two practically relevant settings (a) *expert compression*, i.e. transfer to a student with fewer parameters; and (b) transfer from *privileged experts*, i.e. where the expert has a different observation space than the student, usually including access to privileged information.

1. Introduction

In various control and reinforcement learning settings, there is a need to transfer behavior from an expert policy to a student policy. Broadly, when only samples from the expert policy are available, the standard approach is to employ a version of regression from states to actions. This class of approaches for producing a policy is known as behavioral cloning (Pomerleau, 1989; Michie and Sammut, 1996). Behavioral cloning is quite flexible and supports the setting

where the expert trajectories come from a human teleoperating the relevant system directly, as well as various settings where the trajectories are sampled from other controllers, which themselves may have been trained or scripted. However, for any of the settings where the expert policy is actually available, rather than just samples from the expert, it is reasonable to suspect that sampling random rollouts from the expert policy followed by performing behavioral cloning is not the most efficient approach for transferring behavior from the expert to the student. Once a trajectory has been sampled via an expert rollout, there is actually additional information available that can be ascertained in the neighborhood of the trajectory, without having to perform an additional rollout, via the local feedback properties of the expert.

We refer to this setting, where we want to transfer from an expert policy to a student policy, while assuming the expert policy can be queried, as *policy cloning*. Naturally, there is still often an incentive to reduce the total number of rollouts, which may require actually collecting data in an unsafe or costly fashion, especially for real-world control problems. As such, there is a motivation to characterize any efficiency that can be gained in learning from small numbers of rollouts without as much concern for how many offline queries are required of the expert policy.

If one has primarily encountered behavioral cloning in the context of learning from human demonstrations, policy cloning, with an available expert policy may seem contrived. However, policy cloning naturally arises in many settings. For example, an expert policy may be too large to execute due to memory considerations as in (Parisotto and Salakhutdinov, 2021), where authors propose to distill a large transformer network into small MLPs to be able to execute the policy on data collection workers. In a different setting, we could aim to distill an expert which has access to additional privileged information into a student without access to it, for example by distilling a full state policy into the one which has vision observations. And in the DAGGER setting (Ross et al., 2011), a student policy collects data and is trained by regressing on the expert policy where state distribution comes from the student. In yet another setting, the expert may be suboptimal and the student needs to learn from expert while also being able to exceed the expert performance, perhaps by continuing to learn from a

*Equal contribution ¹DeepMind. Correspondence to: Alexandre Galashov <galashov.alexandr@gmail.com>.

Work was done while at DeepMind. Copyright 2022 by the author(s).

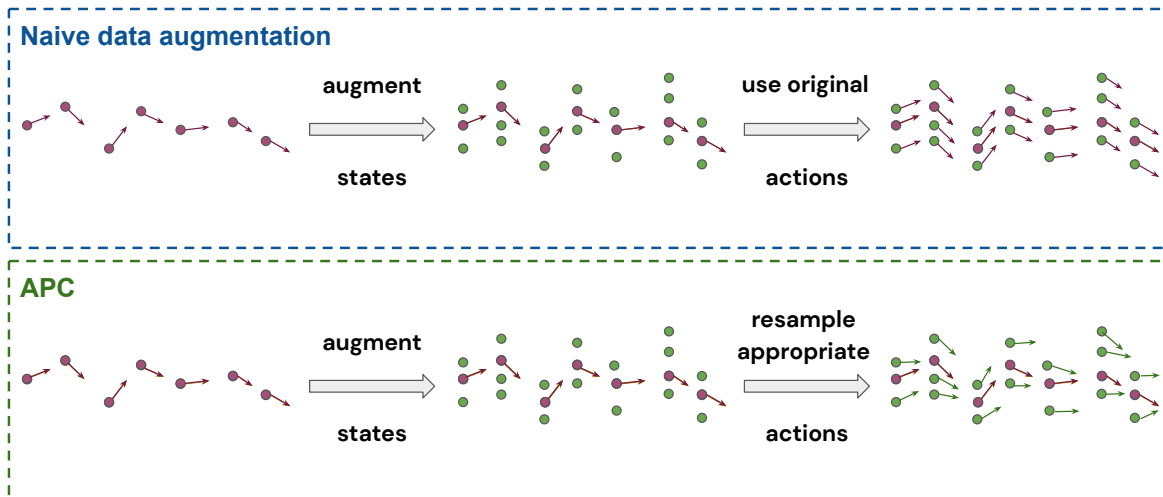


Figure 1. **Schematic of APC** (ours) method compared with a naive data augmentation approach. The original states (magenta circles) and actions (magenta arrows) pairs are then augmented by new virtual states (green circles). In Naive data augmentation, the same actions (magenta arrows) are used for all new virtual states. In APC, however, for each new virtual state, we resample a new action (green arrow) from the expert policy.

task via RL. This problem has been described as *kickstarting* in one incarnation (Schmitt et al., 2018), but also can arise when learning from behavioral priors (Tirumala et al., 2020), (Galashov et al., 2019), as also happens, for example, in Distral (Teh et al., 2017). In all of the aforementioned situations, there is a motivation to minimize the amount of data a student needs to collect.

To improve data-efficiency in supervised settings generally, including in behavioral cloning settings, it is reasonable to consider data augmentation. Data augmentation refers to applying perturbations to a finite training dataset to effectively amplify its diversity, usually in the hopes of producing a model that is invariant to the class of perturbations performed. For example, in the well studied problem of object classification from single images, it is known that applying many kinds of perturbation should not affect the object label, so a model can be trained with many input perturbations all yielding the same output (Shorten and Khoshgoftaar, 2019). This setting is fairly representative, with data augmentation usually intended to make the model “robust” to nuisance perturbations of the input. This class of image-perturbation has also been recently demonstrated to be effective in the context of control problems in the offline RL setting (Yarats et al., 2021; Laskin et al., 2020).

Critically, for control problems it is not the case that the action should be invariant to the input state. Or rather, while it does make sense for a control policy to be invariant to certain classes of sensor noise, an important class of robustness is that the policy is appropriately feedback-responsive. This is to say that for small perturbations of the state of the control system, the optimal action is different in pre-

cisely the way that the expert implicitly knows. This has been recognized and exploited in previous research that has distilled feedback-control plans into controllers (Mordatch and Todorov, 2014; Mordatch et al., 2015; Merel et al., 2019). A similar intuition also underlies schemes which inject noise into the expert during rollouts to sample more comprehensively the space of how the expert recovers from perturbations (Laskey et al., 2017; Merel et al., 2019).

In this work, we leverage this insight to develop a highly efficient policy cloning approach that makes use of both classes of data augmentation. For a high-DoF control problem that operates only from state (humanoid run and insert peg tasks from DeepMind control suite (Tunyasuvunakool et al., 2020)), we demonstrate the feasibility of policy cloning that employs state-based data augmentation with expert querying to transfer the feedback-sensitive behavior of the expert in a region around a small number of rollouts. Then on a more difficult high-DoF control problem that involves both state-derived and egocentric image observations (humanoid running through corridors task from DeepMind control (Tunyasuvunakool et al., 2020)), we combine the state-based expert-aware data augmentation with a separate image augmentation intended to induce invariance to image perturbations. Essentially our expert-aware data augmentation involves applying random perturbations to the state-derived observations, and training the student to match the expert-queried optimal action at each perturbed state, thereby gaining considerable knowledge from the expert without performing excessive rollouts simply to cover the state space around existing trajectories. Our approach compares favorably to sensible baselines, including the naive approach of

attempting to perform behavioral cloning with state perturbations, which seeks to induce invariance (as proposed in Laskin et al., 2020) rather than feedback-sensitivity to state-derived observations. We demonstrate that our approach significantly improves data efficiency on all the settings mentioned above, i.e., behavioral cloning, *expert compression*, cloning *privileged experts*, *Dagger* and *kickstarting*.

2. Problem description

2.1. Expert-driven learning

We start by introducing a notion of expert-driven learning that will be used throughout the paper. At first, we present a general form of the expert-driven objective and then introduce a few concrete examples. We consider a standard Reinforcement Learning (RL) problem. We present the domain as an MDP with continuous states for simplicity, however the problem definition is similar for a POMDP with observations derived from the state. Formally, we describe the MDP in terms of a continuous state space $\mathcal{S} \in \mathcal{R}^n$ (for some $n > 0$), an action space \mathcal{A} , transition dynamics $p(s'|s, a) : \mathcal{S} \times \mathcal{A} \rightarrow p(\mathcal{S})$, and a reward function $r : \mathcal{S} \times \mathcal{A} \rightarrow \mathcal{R}$. Let Π be a set of parametric policies, i.e. of mappings $\pi_\theta : \mathcal{S} \rightarrow p(\mathcal{A})$ from the state space \mathcal{S} to the probability distributions over actions \mathcal{A} , where $\theta \in \mathcal{R}^m$ for some $m > 0$. For simplicity of the notation, we omit the parameter in front of the policy, i.e. $\pi = \pi_\theta$ and optimizing over the set of policies would be equivalent to the optimizing over a set of parameters. A reinforcement learning problem consists in finding such a policy π that it maximizes the expected discounted future reward:

$$J(\pi) = \mathbb{E}_{p(\tau)} \left[\sum_t \gamma^t r(a_t | s_t) \right], \quad (1)$$

where $p(\tau) = p(s_0) \prod_t p(a_t | s_t) p(s_{t+1} | s_t, a_t)$ is a trajectory distribution. We assume the existence of an expert policy $\pi_E(a|s)$. This policy could be used to simplify the learning of a new policy on the same problem. Formally, we construct a new learning objective which aims to maximize the expected reward of the problem at hand as well as to clone the expert policy:

$$J(\pi, \pi_E) = \alpha J(\pi) - \lambda D(\pi, \pi_E), \quad (2)$$

where D is a function which measures the closeness of π to π_E and $\alpha \geq 0, \lambda \geq 0$ are parameters describing importance of both objectives. In most of the applications, $\alpha \in \{0, 1\}$ and $\lambda \geq 0$ represents a relative importance of cloning an expert policy with respect to the RL objective.

2.2. Behavioral cloning (BC)

Behavioral cloning (BC) corresponds to optimizing the objective (2) with $\alpha = 0, \lambda = 1$ and with D defined as:

$$D_{BC}(\pi, \pi_E) = -\mathbb{E}_{(a,s) \in \mathcal{B}_E} [\log \pi(a|s)] \quad (3)$$

Here, $\mathcal{B}_E = \{(s_i, a_i), i = 1, \dots, N\}$, $N > 0$ is a fixed dataset containing expert data. Minimizing the objective (3) is equivalent to maximizing the likelihood of the expert data under the policy π . The action a in eqn. (3) can be replaced by $\pi_E(s)$ for deterministic policies or by the mean $\mu_E(s)$ for Gaussian policies $\pi_E(\cdot|s) = \mathcal{N}(\mu_E(s), \sigma_E(s))$.

2.3. Expert compression

In case of expert compression, we are interested in optimizing a similar objective as in eqn. (3), but where the student π has smaller number of parameters compared to π_E .

2.4. Learning from privileged experts

In case of learning from privileged experts, we optimize similar objective to eqn. (3), where student receives different observations from the expert π_E . We assume that the expert has access to the privileged information, but the student does not. In particular, we consider the case where dataset with expert data contains observations (rather than full state), i.e. $\mathcal{B}_E = \{(o_i, a_i), i = 1, \dots, N\}$, $N > 0$, but the expert has access to the full state s_i . More precisely, we consider an expert that observes the state $s = (s_{common}, s_{priv})$, where s_{common} is a set of observations common to both the student and expert, whereas s_{priv} is privileged information (containing some task-specific information). Then, the observations for the student are obtained as $o = (s_{common}, o_{vis})$ where o_{vis} is the vision-based input.

2.5. DAGGER

Performance of Behavioral Cloning (BC) can be limited due to the fixed dataset, since the resulting policy may fail to generalize to states outside the training distribution. A different approach, known in the literature as DAGGER (Ross et al., 2011) was proposed to overcome this limitation. In this setting, the expert is queried in states visited by the student, thus reducing distribution shift. In our notation, this corresponds to $\alpha = 0, \lambda = 1$ in eqn. (2) and D is defined as:

$$D_{DAGGER}(\pi, \pi_E) = -\mathbb{E}_{p_\beta(\tau)} [\log \pi(a'_t | s_t)], \quad (4)$$

where $p_\beta(\tau)$, $\beta \in [0, 1]$ is a trajectory distribution where actions are sampled according to the mixture policy between a student and an expert:

$$p_\beta(a|s) = \beta \tilde{\pi}(a|s) + (1 - \beta) \pi_E(a|s), \quad (5)$$

The action a'_t in eqn. (4) is obtained from the expert policy as $a'_t \sim \pi_E(\cdot | s_t)$, as $\pi_E(s)$ for deterministic or as $\mu_E(s)$

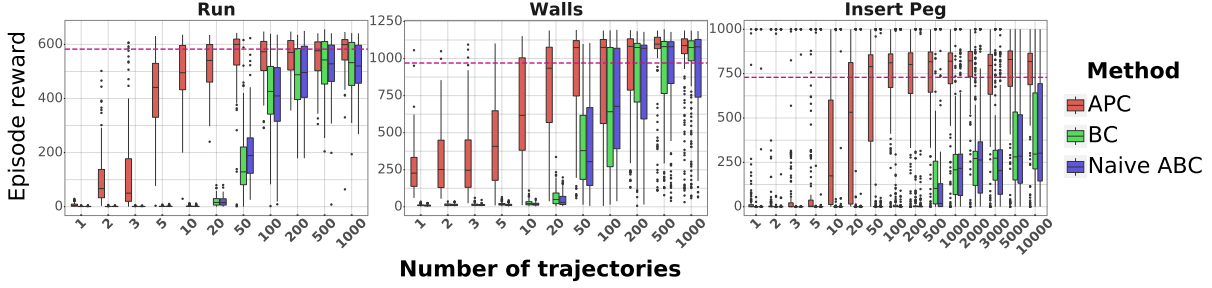


Figure 2. **Offline expert cloning results.** The X-axis represents the number of trajectories, the Y-axis corresponds to the episodic reward across 150 independent evaluations. The red color corresponds to APC, the blue to Naive ABC and the green to BC. The purple line depicts the average performance of the teacher policy. Each subplot represents a different task.

for Gaussian policies $\pi_E(\cdot|s) = \mathcal{N}(\mu_E(s), \sigma_E(s))$ (see Section 2.2). The policy $\tilde{\pi}(a|s)$ corresponds to a frozen version of student policy π so that the gradient $\nabla_{\pi} D_{\text{DAGGER}}(\pi, \pi_E)$ ignores the acting distribution $p_{\beta}(a|s)$. Note that even though, in eqn. (4) we collect data from the environment, the setting nevertheless corresponds to pure imitation learning since expected reward is not directly maximized.

Algorithm 1 Augmented Policy Cloning (APC)

Parametric student policy: π_{θ}
 Initial parameters: θ_0
 Expert policy: π_E
 Dataset $\mathcal{B}_E = \{(s_i, a_i), i = 1, \dots, N\}$, $N > 0$ of expert state-action pairs
 State perturbation noise σ_s
 Learning rate α
 Number of augmented samples: M
 Number of gradient updates: K
 Size of a batch: L
for $k=1, \dots, K$ **do**
 Sample a batch of pairs $\{(a_i, s_i)\}_{i=1}^L \sim \mathcal{B}_E$
 For each state s_i , sample M perturbations $\delta s_j \sim \mathcal{N}(0, \sigma_s)$, $j = 1, \dots, M$
 Construct M virtual states $s'_{i,j} = s_i + \delta s_j$, $i = 1, \dots, L$, $j = 1, \dots, M$
 Resample new actions from expert $a'_{i,j} \sim \pi_E(\cdot|s'_{i,j})$
 For Gaussian experts, the action $a_i = \mu_E(s_i)$ and the new actions are $a'_{i,j} = \mu_E(s'_{i,j})$
 Compute the empirical negative log-likelihood:
 $\mathcal{L} = - \left[\log \pi_{\theta_k}(a_i|s_i) + \frac{1}{M} \sum_{j=1}^M \log \pi_{\theta_k}(a'_{i,j}|s'_{i,j}) \right]$
 Update the parameters $\theta_{k+1} = \theta_k - \alpha \nabla_{\theta} \mathcal{L}$
end for

2.6. Kickstarting

In eqn. (2), we combine both maximization of expected task reward and minimization of distance to the expert. In literature, it is known as *Kickstarting* (Schmitt et al., 2018).

In this case, the objective from eqn. (2) becomes:

$$J(\pi, \pi_E) = J(\pi) - \lambda \mathbb{E}_{p(\tau)} \left[-\mathbb{E}_{\pi_E(a|s)} \log \pi(a|s) \right] \quad (6)$$

where $p(\tau)$ is a trajectory distribution, where actions are sampled according to the student policy $\pi(\cdot|s)$. It corresponds to having $\alpha = 1$, and $\lambda \geq 0$ and D be state-conditional (across trajectory) cross-entropy from expert to a student. Usually, in the *Kickstarting* setting, the expert is sub-optimal and the goal is to train a policy that eventually outperforms the expert. Thus, it is customary to reduce λ over the course of training. Yet, for simplicity, in our experiments we keep this coefficient fixed.

3. Augmented policy cloning

The previous section has demonstrated how the goal of cloning expert behavior can arise in different scenarios. In this section we propose a new and simple method which can significantly improve the data efficiency in the settings described in Section 2. We explain the basic idea for BC, but its generalization to other expert-driven learning approaches described in Section 2 is straightforward. In Section 6 we show results for these problems.

When optimizing the objective (3), for every state $s \in \mathcal{D}_E$ from the expert trajectories dataset, we consider a small Gaussian state perturbation:

$$\delta s \sim \mathcal{N}(0, \sigma_s^2) \quad (7)$$

which produces a new virtual state:

$$s' = s + \delta s \quad (8)$$

Then, for this state we query the expert and obtain a new action

$$a' \sim \pi_E(\cdot|s + \delta s) \quad (9)$$

We then augment the dataset \mathcal{B}_E with these new pairs of virtual states and actions. More explicitly the idea can be

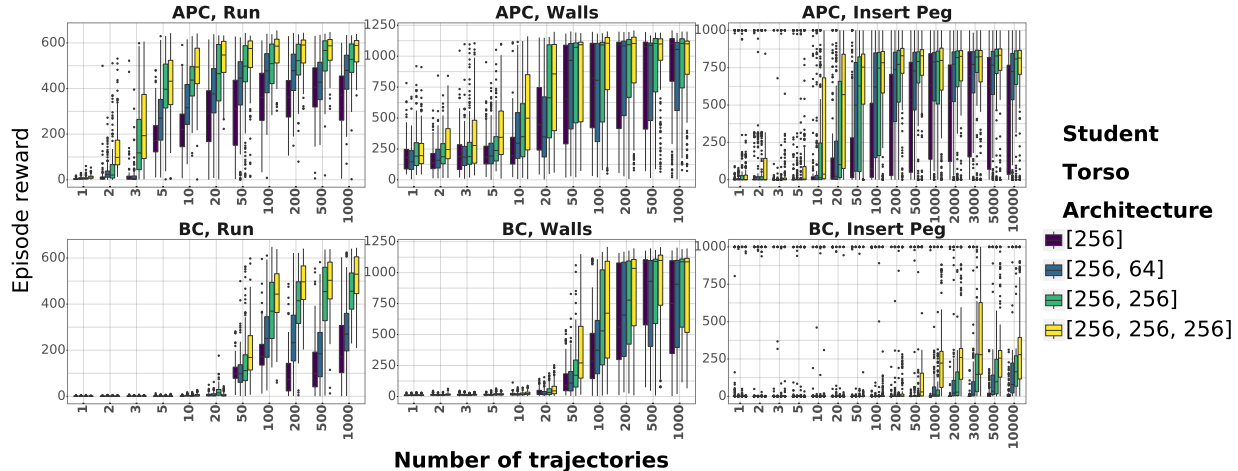


Figure 3. *Teacher compression results.* We plot performances of different methods (rows) on different tasks (columns) as a function of number of trajectories available in the expert dataset. The legend corresponds to different student architectures used. We see that the performance degrades much more drastically for BC compared to APC. We report more complete results in Appendix G.1

expressed in terms of the following objective:

$$D(\pi, \pi_E)_{APC} = \mathbb{E}_{(a,s) \in \mathcal{B}_E} [\log \pi(a|s) + \mathbb{E}_{\delta s \sim \mathcal{N}(0, \sigma_s^2), a' \sim \pi_E(\cdot|s+\delta s)} \log \pi(a'|s+\delta s)] \quad (10)$$

We call this approach *Augmented Policy Cloning (APC)* as it queries the expert policy to augment the training data. This approach is different from a naive data-augmentation technique, where a new state would be generated, but associated with the original action (and not a new one). It therefore allows to build policies which are feedback-responsive with respect to the expert. We illustrate it in Figure 1 and we formulate APC algorithm for BC in Algorithm 1.

4. Experimental details

In this section we provide details common to all experiments. We provide additional details for each set of results at the beginning of Section 5 and Section 6.

4.1. Domains

To study how our method performs on complex control domains, we consider three complex, high-DoF continuous control tasks: *Humanoid Run*, *Humanoid Walls* and *Insert Peg*. All these domains are implemented using the MuJoCo physics engine (Todorov et al., 2012) and are available in the `dm_control` repository (Tunyasuvunakool et al., 2020). These problems are rather challenging, requiring stabilization of a complex body (for humanoid tasks), vision to guide the movement (*Walls* task), and solving a complex control problem with a weak reward signal (*Insert Peg*). These environments are related to the domains that have been proposed for use in offline RL benchmarks (Gulcehre et al., 2020);

however, the experiments we perform in this work require availability of the expert policy, so we do not use offline data, but instead train new experts and perform experiments in the very low data regime. We compare all methods on *Humanoid Run* and *Humanoid Run* tasks and report a subset of results on *Insert Peg*, due to complex nature of the experiments. For more details, please refer to Appendix A.

4.2. Baselines

As baselines we consider simple BC as described in eqn. (3) as well as a simple modification of BC, where, similarly to APC, we apply state perturbations to expert trajectories as in eqn. (7) and eqn. (8), but we do not produce a new action from the expert (i.e., we augment the states but keep the same action). We call this approach *Naive Augmented Behavioral Cloning (Naive ABC)*. Essentially, this method trains a student policy to produce the same action in response to small state perturbations. This approach is motivated by analogy to how one might build robustness in a classifier. However, this is naive when applied to continuous control problems where even small changes in input should lead to a change in action. Moreover, for *Humanoid Walls* task, we considered additional random crops augmentations applied to visual input of the student (not the expert) which is similar in spirit to (Laskin et al., 2020). Note that in this case, it would also robustify the student to these vision augmentations as it will not produce a new action even in the APC (since the expert was not trained with data augmentations). When vision augmentations are used together with either APC or naive ABC, we add "with image" to the method name. When only image augmentations are used (without any state-based augmentations), we call it "image only". The purpose of combining vision and state augmen-

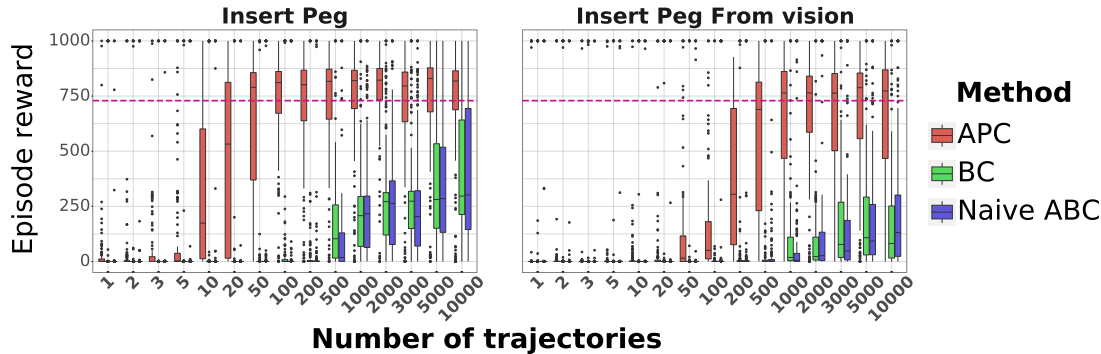


Figure 4. **Learning from privileged experts results.** On the left plot we present the performance of different methods on *Insert Peg* task where additional privileged information (target position) is available. On the right, we present the results where instead of privileged information (target position), we use visual input. We observe that learning from vision is less data efficient and more complicated, but APC manages to obtain comparable performance to the scenario with privileged information, whereas BC and Naive ABC fail to learn.

tations is to study the interplay between APC and more traditional data augmentation methods. We only report results with vision augmentations for *Dagger* and *kickstarting* in the main paper and we provide additional offline policy cloning results in Appendix G.5.

5. Core results: offline policy cloning

Training and evaluation protocols. We train expert policies till convergence using MPO algorithm (Abdolmaleki et al., 2018) for *Humanoid* tasks and VMPO algorithm (Song et al., 2019) for *Insert Peg* task, as we found MPO was unable to learn on this task. The policies are represented by the Gaussian distribution $\pi_E(\cdot|s) = \mathcal{N}(\mu_E(s), \sigma(s))$. We create datasets as in eqn. (3) using pre-trained experts with a different number of expert trajectories. To assess the sensitivity of different methods to the expert noise, when constructing a dataset, the expert action is drawn according to Gaussian distribution with a fixed variance, i.e. $a \sim \mathcal{N}(\mu_E(s), \sigma_E)$, where σ_E is the fixed amount of expert noise. In the subsequent BC experiments, we use $\sigma_E = 0.2$. Moreover, in order to analyze the noise robustness of the student policy is trained via BC, $\pi(\cdot|s) = \mathcal{N}(\mu(s), \sigma(s))$, we evaluate it by executing the action drawn from a Gaussian with a fixed variance, i.e. $a \sim \mathcal{N}(\mu(s), \sigma)$, where σ is the fixed amount of student noise. In all the experiments below we use $\sigma = 0.2$. We apply early stopping and select hyperparameters based on the evaluation performance on a validation set. We always report performance based on 150 random environment instantiations. For more details, see Appendix D.

5.1. Applying Augmented Policy Cloning

We evaluate the performance of APC when fitting the fixed dataset of expert trajectories. For the APC method, we rely on Algorithm 1. We use baselines described in Section 4.2.

In Figure 2, we show the performance of different methods on different tasks as a function of number of trajectories available in the dataset. We see that APC requires significantly fewer expert trajectories to achieve a high level of performance. Moreover, we see that Naive ABC performs very similarly to BC. The results suggest that when cloning an expert using a small fixed set of states APC can provide significant advantages.

In Appendix F, we report additional results for a scenario, where instead of full long trajectories for each task, we consider only short trajectories (i.e., the early portion of episodes). The motivation for this experiment is to see whether we can further improve the data efficiency of the methods. Moreover, in domains where the initial state distribution is randomized in meaningful ways, shorter trajectories can provide an advantage because we get to observe more diverse initial states. Incidentally, this supplemental comparison shows that for *Insert Peg* all methods performed better with short trajectories, because initial snippets of episodes actually include the full solution to the task (i.e., the expert policy rapidly inserts the peg and the episode doesn’t immediately terminate). We report only long trajectories in Figure 2, since APC performs relatively well in both cases and full length trajectories correspond to the most straightforward setting.

5.2. Expert compression

To study APC in a practically motivated setting we consider *expert compression* as discussed in Section 2.3, where a student policy has fewer parameters than the expert. This setting occurs, for instance, when the system is subject to computational constraints (time, memory, etc.), as in (Parisotto and Salakhutdinov, 2021). To study APC’s data efficiency in this setting, we consider different sizes of the student network torso, where $[256, 256, 256]$ corresponds

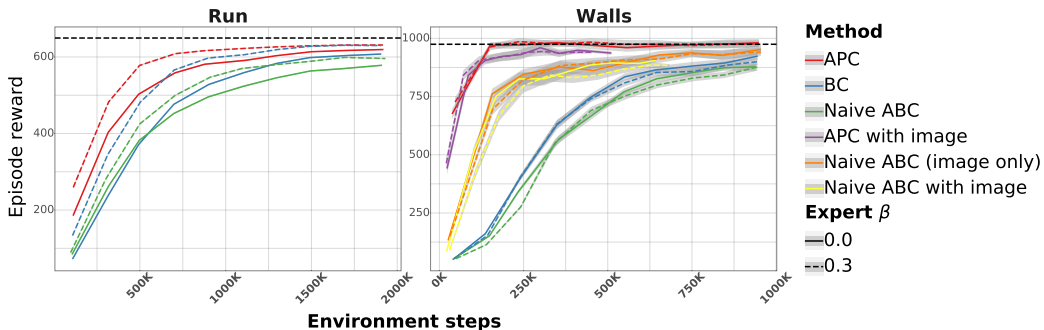


Figure 5. **DAGGER results.** On the X-axis we report the number of environment steps. On the Y-axis we report averaged across 3 seeds episodic reward achieved by the student. We report confidence intervals in the shaded areas. For Run task, the confidence intervals are very small and are not visible. In solid line we report the performance without using expert policy during the acting. In dashed line, we report the performance of the policy which mixes 30% with the expert. All the methods use mean action during evaluation.

to the original network size (see Appendix D.1 for more details).

The results are given in Figure 3. We observe that the performance of all methods degrades when the student network is smaller than the original one, but the degradation is much less severe for APC, while maintaining high level of data efficiency. See Appendix G.1 for more complete results (with naive ABC) as well as additional ablation over student network torso sizes.

5.3. Learning from privileged experts.

Next, we consider a scenario where the expert has access to *privileged information* that is not available to the student, as discussed in Section 2.4. To study the impact of APC in this scenario, we train the expert on *Insert Peg* task where the full state contains common information (proprioception, sword position and orientation) and privileged information of the target position. The student is given access to the common observations as well as a third person (camera) view of the scene providing information about the target position. The latter setup is similar in spirit to (Laskin et al., 2020) For more details, see Appendix D.2.

The results are given in Figure 4. We observe that APC achieves similar performance in both settings, provided a sufficient amount of trajectories are available, whereas BC and Naive ABC fail to transfer the expert’s behavior to the student.

6. Additional Results: Augmented Policy Cloning as a subroutine

6.1. DAGGER with data augmentation

As described in Section 2.5, DAGGER (Ross et al., 2011) is a more sophisticated approach where data is collected from the real environment by executing a policy from eqn. (5),

which is a mixture between a student and an expert. In this section we study how data augmentation approaches affect the data efficiency of the DAGGER algorithm.

For each task, we train expert policies to convergence using the MPO algorithm (Abdolmaleki et al., 2018). We consider similar baselines for both tasks as in the previous section. For an expert policy that has been pre-trained via MPO (Abdolmaleki et al., 2018), we perform online rollouts for two values of the expert-student mixing coefficient, $\beta = 0$ and $\beta = 0.3$ (see eqn. 5). Since both student and expert are Gaussian distributions, instead of using a $\log \pi$ in eqn. (4), we could use a state-conditional cross entropy from an expert to a student, $\mathcal{H}[\pi_E(\cdot|s)||\pi(\cdot|s)]$. Empirically, we found that it worked better than using $\log \pi$ (see Appendix G.6). We run experiments in a data-restricted setup. For more details, see Appendix E.1.

Results are shown in Figure 5. We see that APC and its vision variant outperform BC and Naive ABC similarly to the behavior cloning experiments. While we observe that image augmentation can help, we see that the primary advantage comes from the state-based augmentation for APC. For the Run task, we observe that all DAGGER methods achieve slightly lower performance than an expert policy. We speculate that this is due to insufficient coverage of the state space during training.

6.2. Kickstarting with data augmentation.

A similar in spirit approach is kickstarting (Schmitt et al., 2018), where we solve an RL task as well as cloning the expert policy. Similarly to previous section, we apply APC in kickstarting on the cross entropy term in eqn. (6).

For each task, we train expert policies to convergence using the MPO algorithm (Abdolmaleki et al., 2018). Since in the kickstarting we are interested in outperforming a sub-optimal expert, for each task, we select experts such that

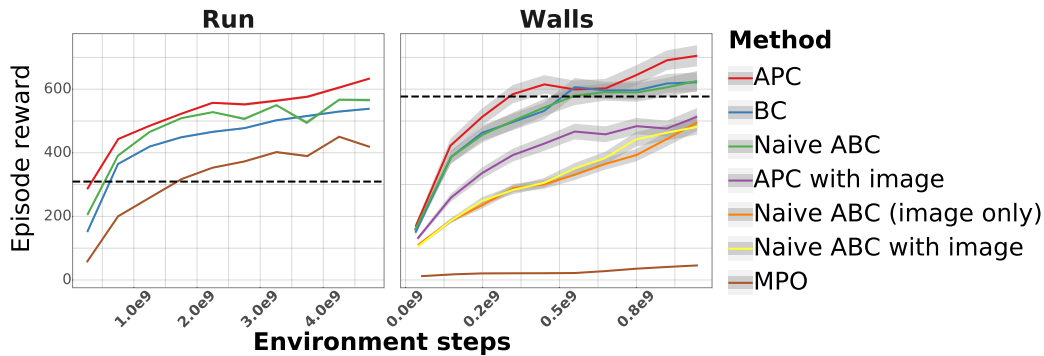


Figure 6. **Kickstarting results.** On the X-axis we show the number of environment steps and on the Y-axis we report averaged across 3 seeds episodic reward achieved by the student. We report confidence intervals in the shaded areas. For Run task, these intervals are small and are not visible. Dashed black line shows the expert performance.

they achieve around 50 % of the optimal performance. On top of kickstarting, we report the performance of MPO (Abdolmaleki et al., 2018) learning from scratch on the task of interest. We run experiment in a distributed, high data regime. All the details are given in Appendix E.2.

The results are given in Figure 6. We observe that APC performs better than Naive ABC on *Humanoid Run* task and similarly on *Humanoid Walls* task. Both approaches perform better than BC and learning from scratch. We hypothesise that the reason of not seeing a consistent advantage could be due several factors. Firstly, as we are in a high-data and distributed regime, since there is no limit on relative acting / learning ratio, and acting policies are not restricted to collect trajectories, it is unclear whether data-augmentation should help. We tried to explore the rate-limiting regime, but we experienced instability of kickstarting experiments. Secondly, we use reward signal which makes the impact of expert cloning less important. Thirdly, on top of learning the policy, we also need to learn an state-action value $Q(s, a)$ function. Unfortunately, we cannot use APC-style data augmentation for learning Q function, therefore it might be the bottleneck. Finally, unlike in kickstarting (Schmitt et al., 2018), we do not use an annealing schedule of λ to make the experiments simpler, but we still observe that a fixed coefficient helps to kickstart an experiment and outperform an expert policy. On top of that, we see that image-based augmentation have less of impact in this setting and generally leads to poor performance.

7. Discussion

Many expert-driven learning approaches actually have access to an expert that can be queried; however, this opportunity is rarely exploited fully. In this work we demonstrated a general scheme for more efficient transfer of expert behavior by augmenting expert trajectory data with virtual, perturbed states as well as the expert actions in these virtual states.

This data augmentation technique is widely applicable and we demonstrated that it improves data efficiency when used in place of behavioral cloning in various settings including offline cloning, expert compression, transfer from privileged experts, or when behavioral cloning is used as a subroutine within online algorithms such as DAGGER or kickstarting.

Critically, data efficiency is generally very important in realistic applications, where new data acquisition cost could be high. In particular, settings involving deployment of policies in the real world, such as robotics applications, may benefit from an ability to efficiently transfer expert policy behavior from one neural network to another (for compression or execution speed reasons). While overall, we consider the present work to be fairly basic research with limited ethical impact, insofar as our approach decreases the amount of data which needs to be collected through processes which could potentially be unsafe or costly, there is a potential positive social value.

Our approach is neither intended for nor suitable for all control settings. Fundamentally, our approach relies upon the ability to query expert policy for the perturbed states. This arises frequently enough to be worth our investigation, but is a limiting assumption. Our approach was also developed with continuous control problems, essentially with continuous observation spaces as well as continuous action spaces in mind. Related approaches may be worth pursuing in discrete control problems, but that has not been a focus of the present work.

An interesting future direction would be to explore different ways we could generate virtual states. Even though simple Gaussian perturbation of states seems to work fairly well, we could explore a possibility of building a state model and sample the virtual states from it.

References

- Abbas Abdolmaleki, Jost Tobias Springenberg, Yuval Tassa, Remi Munos, Nicolas Heess, and Martin Riedmiller. Maximum a posteriori policy optimisation, 2018.
- Alexandre Galashov, Siddhant M. Jayakumar, Leonard Hasenclever, Dhruva Tirumala, Jonathan Schwarz, Guillaume Desjardins, Wojciech M. Czarnecki, Yee Whye Teh, Razvan Pascanu, and Nicolas Heess. Information asymmetry in kl-regularized rl, 2019.
- Caglar Gulcehre, Ziyu Wang, Alexander Novikov, Thomas Paine, Sergio Gómez, Konrad Zolna, Rishabh Agarwal, Josh S Merel, Daniel J Mankowitz, Cosmin Paduraru, et al. Rl unplugged: A collection of benchmarks for offline reinforcement learning. *Advances in Neural Information Processing Systems*, 33, 2020.
- Matt Hoffman, Bobak Shahriari, John Aslanides, Gabriel Barth-Maron, Feryal Behbahani, Tamara Norman, Abbas Abdolmaleki, Albin Cassirer, Fan Yang, Kate Baumli, Sarah Henderson, Alex Novikov, Sergio Gómez Colmenarejo, Serkan Cabi, Caglar Gulcehre, Tom Le Paine, Andrew Cowie, Ziyu Wang, Bilal Piot, and Nando de Freitas. Acme: A research framework for distributed reinforcement learning, 2020.
- Michael Laskey, Jonathan Lee, Roy Fox, Anca Dragan, and Ken Goldberg. Dart: Noise injection for robust imitation learning. In *Conference on robot learning*, pages 143–156. PMLR, 2017.
- Michael Laskin, Kimin Lee, Adam Stooke, Lerrel Pinto, Pieter Abbeel, and Aravind Srinivas. Reinforcement learning with augmented data, 2020.
- Josh Merel, Leonard Hasenclever, Alexandre Galashov, Arun Ahuja, Vu Pham, Greg Wayne, Yee Whye Teh, and Nicolas Heess. Neural probabilistic motor primitives for humanoid control, 2019.
- Donald Michie and Claude Sammut. *Behavioural Clones and Cognitive Skill Models*, page 387–395. Oxford University Press, Inc., USA, 1996. ISBN 019853860X.
- Igor Mordatch and Emo Todorov. Combining the benefits of function approximation and trajectory optimization. In *Robotics: Science and Systems*, volume 4, 2014.
- Igor Mordatch, Kendall Lowrey, Galen Andrew, Zoran Popovic, and Emanuel V Todorov. Interactive control of diverse complex characters with neural networks. *Advances in Neural Information Processing Systems*, 28: 3132–3140, 2015.
- Emilio Parisotto and Ruslan Salakhutdinov. Efficient transformers in reinforcement learning using actor-learner distillation, 2021.
- Dean A Pomerleau. Alvin: An autonomous land vehicle in a neural network. Technical report, Carnegie-Mellon, 1989.
- Stephane Ross, Geoffrey J. Gordon, and J. Andrew Bagnell. A reduction of imitation learning and structured prediction to no-regret online learning, 2011.
- Simon Schmitt, Jonathan J. Hudson, Augustin Zidek, Simon Osindero, Carl Doersch, Wojciech M. Czarnecki, Joel Z. Leibo, Heinrich Kuttler, Andrew Zisserman, Karen Simonyan, and S. M. Ali Eslami. Kickstarting deep reinforcement learning, 2018.
- Connor Shorten and Taghi Khoshgoftaar. A survey on image data augmentation for deep learning. *Journal of Big Data*, 6, 07 2019. doi: 10.1186/s40537-019-0197-0.
- H. Francis Song, Abbas Abdolmaleki, Jost Tobias Springenberg, Aidan Clark, Hubert Soyer, Jack W. Rae, Seb Noury, Arun Ahuja, Siqi Liu, Dhruva Tirumala, Nicolas Heess, Dan Belov, Martin Riedmiller, and Matthew M. Botvinick. V-mpo: On-policy maximum a posteriori policy optimization for discrete and continuous control, 2019.
- Yee Whye Teh, Victor Bapst, Wojciech Marian Czarnecki, John Quan, James Kirkpatrick, Raia Hadsell, Nicolas Heess, and Razvan Pascanu. Distral: Robust multitask reinforcement learning. *arXiv preprint arXiv:1707.04175*, 2017.
- Dhruva Tirumala, Alexandre Galashov, Hyeonwoo Noh, Leonard Hasenclever, Razvan Pascanu, Jonathan Schwarz, Guillaume Desjardins, Wojciech Marian Czarnecki, Arun Ahuja, Yee Whye Teh, et al. Behavior priors for efficient reinforcement learning. *arXiv preprint arXiv:2010.14274*, 2020.
- Emanuel Todorov, Tom Erez, and Yuval Tassa. Mujoco: A physics engine for model-based control. In *2012 IEEE/RSJ International Conference on Intelligent Robots and Systems*, pages 5026–5033. IEEE, 2012.
- Saran Tunyasuvunakool, Alistair Muldal, Yotam Doron, Siqi Liu, Steven Bohez, Josh Merel, Tom Erez, Timothy Lillicrap, Nicolas Heess, and Yuval Tassa. dm_control: Software and tasks for continuous control. *Software Imprints*, 6:100022, 2020.
- Denis Yarats, Ilya Kostrikov, and Rob Fergus. Image augmentation is all you need: Regularizing deep reinforcement learning from pixels. In *9th International Conference on Learning Representations, ICLR*, volume 2021, 2021.

A. Environment details

In this work we consider three environments from DeepMind Control repository (Tunyasuvunakool et al., 2020): *Humanoid Run*, *Humanoid Walls* and *Insert Peg*. *Humanoid Run* task requires an agent controlling humanoid body to run at a specific speed and gets reward which is proportional to the inverse distance between its current speed and the target speed. The observations are based on proprioceptive information. In *Humanoid Walls*, an agent controls a humanoid body to run along a corridor and avoid walls, at highest possible speed. The observations are based on proprioception and on egocentric vision. It receives reward which is proportional to the forward speed (through the corridor), thus incentivising it to run as fast as possible. It receives proprioceptive observations as well as the image of size 64x64 from the ego-centric camera. In our experiments, we use *Simple Humanoid* body rather than *CMU Humanoid* as in the original task in order to simplify the experiments. Action dimension is equal to 21. Finally, in *Insert Peg*, an agent controls an arm which needs to put a sword into a narrow hole. The observations are based on proprioception, sword position and orientation, hole position. In case of vision-based input, we add second person camera observations with image size of 64x64. For more details, check (Tunyasuvunakool et al., 2020). Note these environments are related to the domains that have been proposed for use in offline RL benchmarks (Gulcehre et al., 2020); however, the experiments we perform in this work require availability of the expert policy, so we do not use offline data, but instead train new experts and perform experiments in the very low data regime. We choose these exact environments due to their challenging nature in order to demonstrate the impact of APC on data efficiency, but we did try initially simpler environments from the DeepMind Control repository (Tunyasuvunakool et al., 2020) which included *Humanoid Walk* and *Walker Walk/Run* tasks. We decided not to conduct exhaustive experiments on these environments.

B. Methods and baselines

The main method we consider is APC described in Section 3 for offline experts cloning experiments. For all the methods in offline expert cloning experiments, as an action in the objective from eqn. (3), we use an expert mean $\mu_E(s)$. We also extend this method to scenarios from Section 6, i.e. on DAGGER and kickstarting. For both scenarios, applying APC is straightforward. In case of DAGGER, the APC approach would correspond to resampling additional states via eqn. (7) and via eqn. (8) for each state s_t encountered in the objective from the eqn. (4). Then, for each such new state $s' = s_t + \delta s$, we would add a term to optimize in the objective, corresponds to the cross entropy from the expert to the student, i.e. $\mathcal{H}[\pi_E(\cdot|s')||\pi(\cdot|s')]$. We can also consider resampling a new action, but we empirically found that cross-entropy worked better, see Appendix (G.6). For kickstarting, applying APC would also correspond to sampling new virtual states $s' = s + \delta s$ for each state in the second term of the eqn. (6). Then similarly, we would add an additional cross entropy term to the objective, i.e., $\mathcal{H}[\pi_E(\cdot|s')||\pi(\cdot|s')]$.

As baselines against APC, we consider BC algorithm described in eqn. (3), which in DAGGER and kickstarting simply corresponds to the unmodified versions of this method. On top of BC, we consider a simple modification of BC, where we apply, similar to APC, state perturbations to expert trajectories as in eqn. (7) and eqn. (8), but we do not produce a new action from the expert and use the original one. We call this approach Naive Augmented Behavioral Cloning (Naive ABC). Essentially, this method trains a student policy to be robust with respect to small state perturbations. The application of Naive ABC in case of DAGGER and kickstarting is similar to APC, with the exception that we now consider the cross entropy term $\mathcal{H}[\pi_E(\cdot|s)||\pi(\cdot|s')]$, where the student is taken on the new augmented states and the expert on the original, unmodified ones.

Moreover, for *Humanoid Walls* task, we considered additional vision-based augmentations, random crops, similar in spirit to (Laskin et al., 2020). Note that in this case, it would also robustify the student to these vision augmentations as it will not produce a new action even in the APC (since the expert was not trained with data augmentations). When vision augmentations are used together with APC or naive ABC, we add "with image" to the method name. When only image augmentations are used (without any state-based augmentations), we call it "image only". The purpose of combining vision and state augmentations is to study the interplay between APC and more traditional data augmentation methods. We use random crops producing images of size 48x48 instead of the original 64x64 images.

C. Agent architecture

For all the experiments, we use the same agent architecture. The agent has two separate networks: actor (policy) and critic (Q-function). Both networks are split into 3 components: encoder, torso and head. Encoders for actor and critic are separate

but have the same architecture. For state-only (no vision) observations, encoder corresponds to a simple concatenations of all the observations. For the visual input, it divides each pixel by 255 and then applies a 3-layer ResNet of sizes (16, 32, 32) with *ELU* activations followed by a linear layer of size 256 and *ELU* activation. The resulting output is then concatenated together with state-based input. For actor network, torso corresponds to a 3 dimensional MLP, each hidden layer of size 256 with activation *ELU* applied at the end of each hidden layer. The output of actor torso is then passed to the actor head network, which applies a linear layer (without activation) with output size equal to $N_a * 2$, where N_a is the action dimension. It produces the actor mean μ and log-variance: $\log \tilde{\sigma}$. Then, the variance of the actor is calculated as

$$\sigma = \text{softplus}(\log \tilde{\sigma}) + \sigma_{min},$$

where $\sigma_{min} = 0.0001$. That would encode the Gaussian policy $\pi(\cdot|s) = \mathcal{N}(\mu(s)|\sigma(s))$. This parameterization ensures that the variance is never 0. The critic torso network is 1 dimensional MLP of size 256 with *ELU* activation on top of it. Both critic encoder and critic torso are applied to the state input and not the action. The output of torso and the action are passed to the head, which firstly applies a *tanh* activation to the action to scale it in $[-1, 1]$ interval, then concatenates both scaled action and torso output. This concatenated output is then passed through a 3-dimensional MLP with sizes [256, 256, 1] with *ELU* activations applied to all layers except the last one. This produces the Q-function representation, $Q(s, a)$. The critic network is not used for the offline expert cloning and DAGGER experiments.

To train experts for *Humanoid Run* and *Humanoid Walls* tasks, we use MPO (Abdolmaleki et al., 2018) algorithm with default hyperparameters. For *Insert Peg* experiments, we use VMPO (Song et al., 2019) algorithm since we found that MPO (Abdolmaleki et al., 2018) failed to train. We use the same architecture as described above and use default hyperparameters from VMPO original paper.

D. Offline policy cloning experiment details

For each task, we train expert policies till convergence. We use MPO algorithm (Abdolmaleki et al., 2018) for *Humanoid* tasks and VMPO algorithm (Song et al., 2019) for *Insert Peg* task, as we found MPO was unable to learn on this task.

The policies are represented by the Gaussian distribution $\pi_E(\cdot|s) = \mathcal{N}(\mu_E(s), \sigma(s))$. We create datasets as in eqn. (3) using pre-trained experts with a different number of expert trajectories. To assess the sensitivity of different methods to the expert noise, when constructing a dataset, the expert action is drawn according to Gaussian distribution with a fixed variance, i.e.

$$a \sim \mathcal{N}(\mu_E(s), \sigma_E), \quad (11)$$

where σ_E is the fixed amount of expert noise. We consider 4 different levels of σ_E : **Deterministic**, meaning that we unroll the expert trajectories using only the mean μ_E , **Low**: $\sigma_E = 0.2$, **Medium**: $\sigma_E = 0.5$, **High**: $\sigma_E = 1.0$. We also tried values in-between, but did not find a qualitative difference. We also tried values above $\sigma_E = 1.0$, but the performance for these ones was almost zero. In all the experiments, we use $\sigma_E = 0.2$. We provide additional ablation over different levels of expert noise σ_E in Appendix G.3.

We unroll the expert trajectories by chunks containing 10 time steps each and put it in a dataset. We use Reverb (from ACME (Hoffman et al., 2020)) backend for this. A full trajectory for a *Humanoid Run* task corresponds to 1000 time steps which corresponds to 25 seconds of control time with a control discretization of 0.025 seconds. A full trajectory for a *Insert Peg* task corresponds to 1000 time steps which corresponds to 10 seconds of control time with a control discretization of 0.1 seconds. A full trajectory for the *Humanoid Walls* task corresponds to 2000-2500 time steps. This variation is due to potential early stopping of the task execution (in case if the agent falls down). The discretization for the control is 0.03 seconds and maximum episode length is 45 seconds.

For each task, we construct datasets containing 1, 2, 3, 5, 10, 20, 50, 100, 200, 500, 1000 trajectories. For *Insert Peg* task, we also create datasets containing 2000, 3000, 5000 and 10000 trajectories, as we found this task requiring more data to be able to be learned.

When evaluating the method, in order to analyze the noise robustness of the student policy is trained via BC, $\pi(\cdot|s) = \mathcal{N}(\mu(s), \sigma(s))$, we evaluate it by executing the action drawn from a Gaussian with a fixed variance, i.e.

$$a \sim \mathcal{N}(\mu(s), \sigma), \quad (12)$$

where σ is the fixed amount of student noise. We tried similar value for σ as in case of expert noise σ_E . In all the experiments below we use $\sigma = 0.2$. We provide additional ablation over these values in Appendix G.3.

To train offline expert cloning methods we rely on Algorithm 1 as the main algorithm for all the methods, where we remove additional action or/and state augmentations for Naive ABC and BC. For all the experiments we use learning rate $\alpha = 0.0001$, number of augmented samples $M = 10$, batch size $L = 64$. We did try different values for these parameters and found it made no difference on the performance and final experiments outcome, so we fixed one set of parameters for the simplicity of the experimentation.

For every method and task, we tune method-specific hyperparameters. It corresponds to tuning state noise perturbation variance σ_s^2 from eqn. (7) for APC and Naive ABC (we do not need to tune it for BC as we do not use any data augmentation in case of BC). The considered range for this parameter is $[0.0001, 0.001, 0.01, 0.05, 0.1, 1.0, 10.0]$. For APC, we found that $\sigma_s = 0.1$ worked best for *Humanoid Run* and *Insert Peg*, and $\sigma_s = 1.0$ worked best for *Humanoid Walls* task. For Naive ABC, these values are: $\sigma_s = 0.001$ for *Humanoid Run*, $\sigma_s = 0.01$ for *Insert Peg* and $\sigma_s = 0.0001$ for *Humanoid Walls* tasks. We select these parameters based on the validation set performance in the procedure described in the next paragraph. We use the same values of σ_s for vision-based augmentation variants as the original method to which these vision-based augmentations are applied. For example, if the method is APC with image, it means that we use σ_s for APC in this experiment.

We train all the offline expert cloning methods till convergence (maximum 20M iterations) for each experiment / task / method variant. Each iteration corresponds to applying gradients to the batch of 64 trajectories, each containing 10 time steps. We evaluate each model using 150 random environment instantiations. We noticed that when we train models offline, at convergence there are small variations in performance among subsequent models. Therefore, we use early stopping to select for the best model for each experiment. In order to do that, we use a validation set of separate 50 random environment instantiations and we select the best model based on the average performance among these 50 instantiations. We use the same early stopping procedure to select for the best hyperparameter.

D.1. Expert compression: details

We consider *expert compression* setting as discussed in Section 2.3, where a student policy has smaller parameters than the expert. This setting often occurs in situations where there are computation constraints (memory, etc.) on the system which would be used on the student as in (Parisotto and Salakhutdinov, 2021). To study the APC data efficiency in this setting, we consider different sizes of the student network torso, where $[256, 256, 256]$ corresponds to the original network size. In particular, we consider following sizes: $[256]$, $[256, 64]$, $[256, 256]$. We consider additional network sizes and provide additional ablations in Appendix G.1.

D.2. Learning from privileged experts: details

We consider a scenario where the expert has access to the *privileged information* whereas student does not, as discussed in Section 2.4. Typically, in such a scenario, it is easier to train the expert than the student, but training a student with a restricted observations is more preferable in an application.

To study the impact of APC in this scenario, we train the expert on *Insert Peg* task where the full state contains common information (proprioception, sword position and orientation) and privileged information of the target position. The student is then trained on the common observations and on vision-based input through the second person camera which replaces privileged information. The latter setup is similar in spirit to (Laskin et al., 2020). The student network with additional vision observations therefore has an additional visual input encoder as described in Appendix C. It encodes non-vision observations with simple concatenation and concatenates the result with the vision embedding. It is then passed through the same torso and head networks as original expert. In this regime, the student does not know about the target position and needs to infer it from vision-based observations.

E. APC as subroutine: experimental details

E.1. DAGGER experiment details

For each task, we train expert policies to convergence using the MPO algorithm (Abdolmaleki et al., 2018). Each expert is represented by a Gaussian policy, see Appendix C. Throughout the experiment, we use the replay buffer of size $1e6$ where each element corresponds to 10-step trajectory, implemented using Reverb (from ACME (Hoffman et al., 2020)). We use the actor-learning architecture, with 1 actor and 1 learner, where the actor focuses on unrolling current policy and on collecting

the data, whereas the learner samples the trajectories from the replay buffer and applies gradient updates on the parameters. When doing so, we control a relative rate of acting / learning via rate limiters as described in (Hoffman et al., 2020) such that for each time step in the trajectory, we apply in average 10 gradient updates. This allows us to be very data efficient and get the full power from the data augmentation technique. In order to achieve it, we set the samples per request (SPI) parameter of the rate limiter to be $T * B * 10$, where $T = 10$ is the trajectory length (sample from a replay buffer), B is the batch size (256 for Run and 32 for Walls). When sampling from the replay buffer, we use uniform sampling strategy. When the replay buffer is full, the old data is removed using FIFO-strategy.

For each method and each domain, we run the experiment with 3 random seeds. Normally, in DAGGER, the parameter β of mixing the experience between the student and an expert, should decrease to 0 throughout the learning. For simplicity of experimentation, we used fixed values. We report the results using $\beta = 0$ and $\beta = 0.3$, but we also experimented with values $\beta = 0.1, 0.2, 0.4, 0.5$. We found that our chosen values provided most of the qualitative information. The values of state perturbation noise for APC are: $\sigma_s = 0.1$ for Run and $\sigma_s = 1.0$ for Walls task. For Naive ABC, these values are: $\sigma_s = 0.01$ for Run and $\sigma_s = 0.001$ for Walls tasks. The values which we tried are: $[0.00001, 0.0001, 0.001, 0.01, 0.1, 1.0, 10.0]$.

When collecting the data, we use a mixture of student and expert, which are represented as stochastic policies via Gaussian distributions. For evaluation, we used their deterministic versions, by unrolling only the mean actions.

To train policies via DAGGER, we used analytical cross-entropy between expert and student instead of log probability of student on expert mean actions, as we found that it worked better in practice. We provide qualitative comparison in Appendix G.6.

E.2. Kickstarting experiment details

For each task, we train expert policies to convergence using the MPO algorithm (Abdolmaleki et al., 2018). Since in the kickstarting we are interested in outperforming sub-optimal expert, we select experts which achieve around 50 % of optimal performance on each task. Each expert is represented by a Gaussian policy, see Appendix C. We run experiments using a distributed setup with 64 actors and 1 learner, which queries the batches of trajectories (each containing 10 time steps) from a replay buffer of size $1e6$. We use Reverb (from ACME (Hoffman et al., 2020)) as a backend. Batch size is 256 for Run and 32 for Walls. We run the sweep over λ parameter from eqn. (6) from the main paper. As opposed to DAGGER, we do not use the rate-limiter to control the relative ratio between acting and learning as we found that kickstarting in such a regime was unstable. We found that $\lambda = 0.0001$ worked best for Run, whereas $\lambda = 0.01$ worked best for Walls. The values we tried are: $[0.0001, 0.001, 0.01, 0.1, 1.0, 10.0]$. We found that for higher values of λ , the learning was faster but the resulting policy did not outperform the expert. On top of running BC methods, we also report the performance of MPO (Abdolmaleki et al., 2018) learning from scratch on the task of interest. The values of state perturbation noise for APC are: $\sigma_s = 0.01$ for Run and $\sigma_s = 0.01$ for Walls task. For Naive ABC, these values are: $\sigma_s = 0.00001$ for Run and $\sigma_s = 0.0001$ for Walls tasks. The values which we tried are: $[0.00001, 0.0001, 0.001, 0.01, 0.1, 1.0, 10.0]$. On top of that, when using the MPO algorithm during kickstarting, we modify MPO-specific parameters ϵ_μ and ϵ_Σ to $\epsilon_\mu = 0.05$ and $\epsilon_\Sigma = 0.001$ as we found that using higher values for M-step constraints led to better kickstarting performance. When we apply image-augmentations for kickstarting, we only apply it on the student policy and not on student Q -function. Empirically, we found that adding image augmentations for Q function inputs led to worse performance.

E.3. Plotting details

When we plot the results in Figure 5, Figure 6, Figure 15 and Figure 16 we use the following method. For each independent task, method and independent run (seed), we split the data into bins, each containing 10% of the data. Then, in each bin, the performance is averaged as well as the 95% confidence interval is calculated. We then report these values in the figure.

F. Short trajectories experiment

In this section we present additional results to the ones presented in Section 5. We discussed that we construct the dataset of expert trajectories containing full trajectories (1000 timesteps for *Humanoid Run* and *Insert Peg* and around 2000 timesteps for *Humanoid Walls*). It corresponded to a simple unroll of the expert policy on the original environments. In addition to that, we create datasets which contain only one full trajectories and a given number of short trajectories, where each short trajectory contains only 200 timesteps starting from the initial state. The reason for this experiment is to study the ability of different offline expert cloning methods for a more data restricted setup. Note that such a scenario can occur in practice

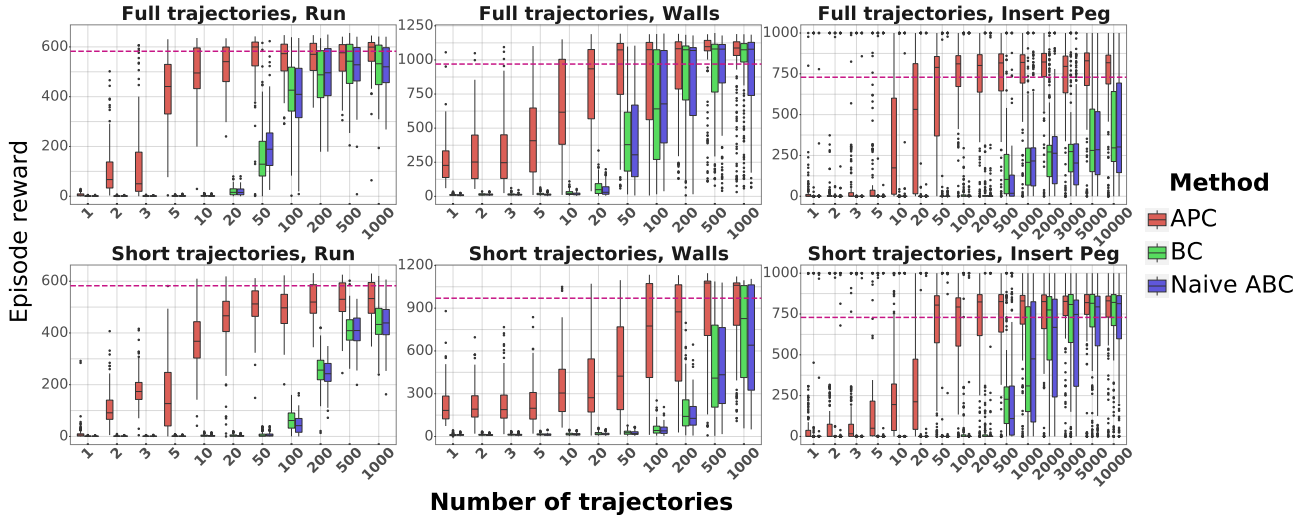


Figure 7. Offline expert cloning results with different number of trajectories for APC, BC and Naive ABC on *Humanoid Run*, *Humanoid Walls* and *Insert Peg* tasks represented by columns. First row corresponds to the full trajectory case, as reported in Figure 2. Second row corresponds to the case of short trajectories, where the dataset contain one full and a given number of short trajectories. The X-axis represents the number of trajectories, the Y-axis corresponds to the episodic reward across 150 independent evaluations.

when dealing with realistic robots, where dataset can contain a lot of successful trajectories, but the trajectories can be short, because a robot can fail at some points of time.

We present results in Figure 7, where we duplicate the results for full trajectories and add additional results for short trajectories. We observe that APC performs well in all the cases, whereas BC and Naive ABC performance degrade on *Humanoid Run* and on *Humanoid Walls*. What is interesting, however, is that these methods perform better on *Insert Peg* scenario with short trajectories (but still worse than APC). The reason for is due to the fact that in *Insert Peg*, the rewarding state corresponds to a situation where arm inserted a sword into a hole and does not move (and episode is not finished until 1000 time steps had elapsed). Therefore, long trajectories of expert policies will contain a lot of such states and actions, therefore having a limited diversity. In case of short trajectories, the relative ratio of states preceding this final state is much higher. Interestingly, APC still performs well in both scenarios.

G. Ablations

G.1. Expert compression additional results

In this section we present additional results for *expert compression* experiment from Section 2.3.

Firstly, we present an ablation over different network sizes in Figure 8. We see that generally APC degrades much less than other methods when we decrease the student network size.

Secondly, as an additional to the results in Figure 3, we present results for all the tasks and all the methods on Figure 9

G.2. Learning from privileged experts: additional results

We present additional results to the experiment presented in Section 2.4 where we also consider *Insert Peg* tasks where dataset contains only short trajectories as we have seen in Appendix F that all methods performed better on this task with short trajectories. The results are given in Figure 10.

G.3. APC expert noise sensitivity

In this section we present additional ablations on the sensitivity of APC, BC and Naive ABC to different values of expert noise σ_E from eqn. (11) and student noise σ from eqn. (11). We consider four different levels of noise as discussed in

Data augmentation for efficient learning from parametric experts

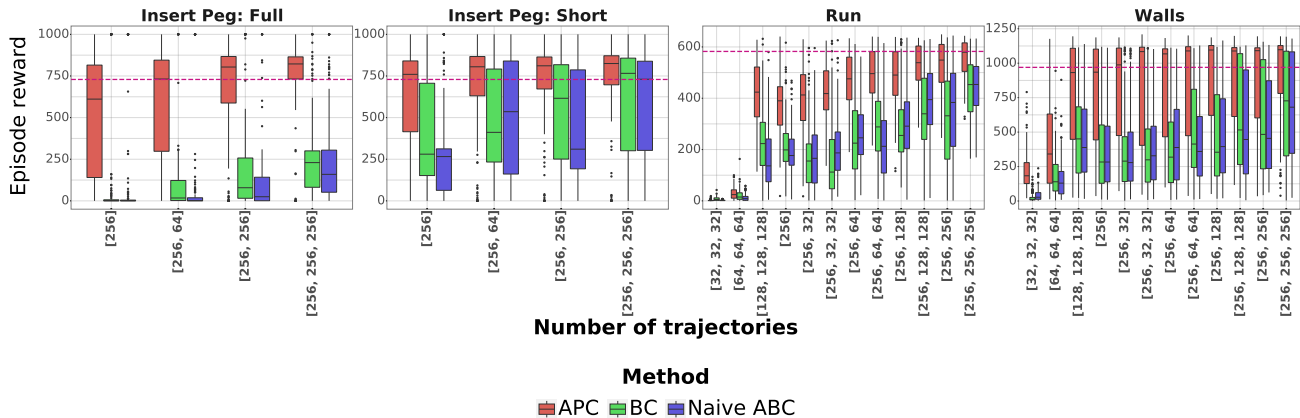


Figure 8. Teacher compression results with additional student torso architecture sizes.

Appendix D. The results are given in Figure 11. For *Humanoid Run* and *Humanoid Walls* tasks, we use 100 trajectories dataset, whereas for *Insert Peg*, we use dataset with 2000 trajectories, as this task is much less data efficient than others. Moreover, for *Insert peg* we consider scenario with full and short trajectories, whereas for *Humanoid* tasks we consider only full trajectories. We see that overall, APC provides more robust policies for different amounts of expert and student noise. For expert noise sensitivity, note that over different columns, the APC performance degrades much less than for BC and Naive ABC. Moreover, for each column, observing the change of the student noise level (from low to high), we see that performance degrades for all the methods, but much less for APC. Therefore, APC seems to provide more action-noise robust policies. We see that BC and Naive ABC perform similarly in terms of robustness. Finally, what is interesting, APC generally observes much less variance in performance when varying the noise levels compared to BC and Naive ABC

G.4. APC and ABC state noise ablations

In this section we provide additional ablations for the state-noise perturbation level σ_s from the eqn. (7) from the main paper. In Figure 12, we show the results for APC, whereas in Figure 13, we show the results for Naive ABC. We see that there is a sweet spot for the state perturbation noise level.

G.5. Additional comparisons for Walls task

In Figure 14, we provide additional results for behavioral cloning experiment on Walls task where we try different variants of APC and Naive ABC with additional image-based augmentation as described in the main paper.

G.6. Objective functions comparison for DAGGER

In Figure 15 and in Figure 16, we provide ablations over different objectives for DAGGER with $\beta = 0.0$ and $\beta = 0.3$ correspondingly. We see that overall, training with cross-entropy leads to better results than with log prob on the mean action, especially when $\beta = 0.0$.

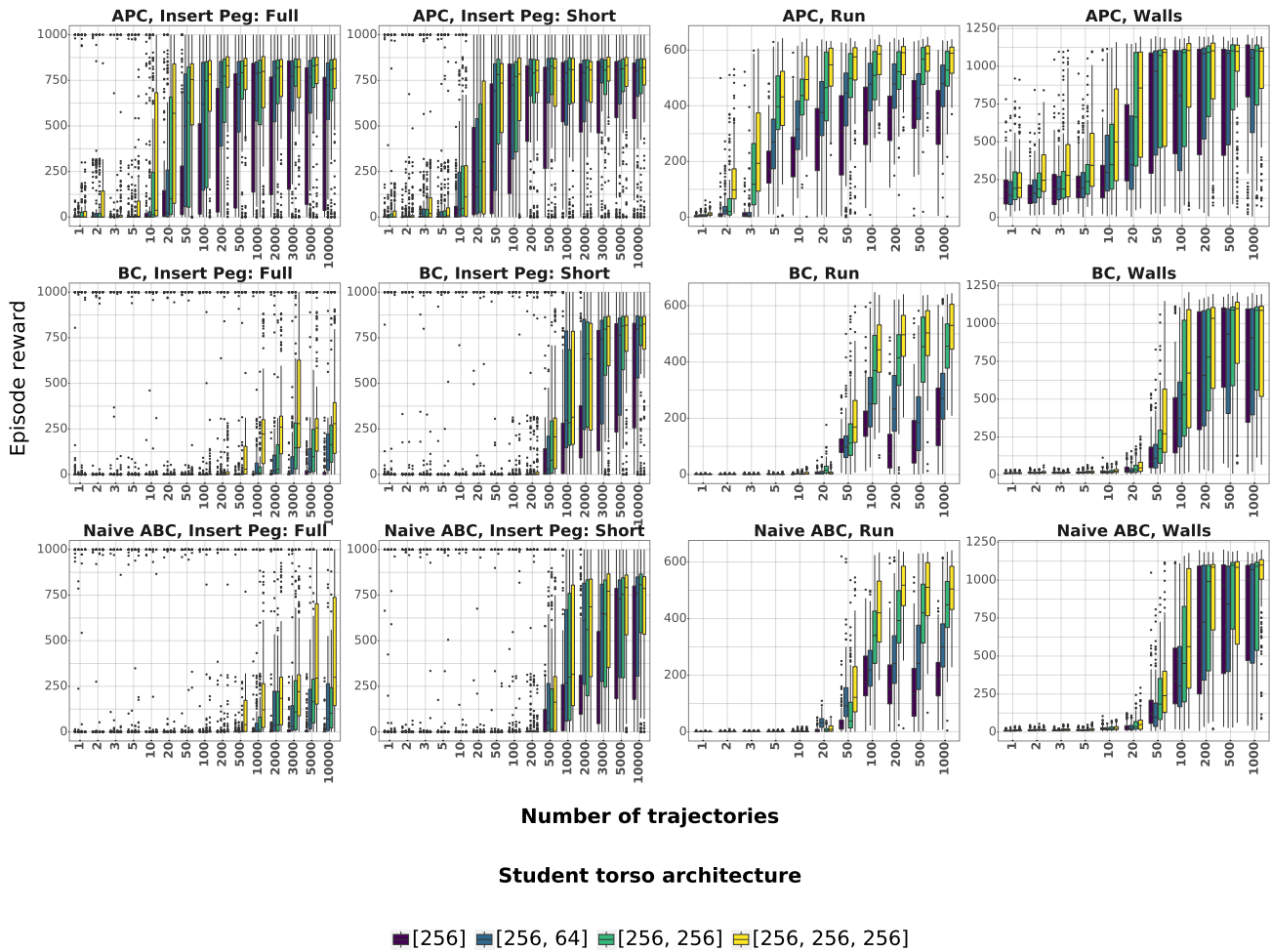


Figure 9. Teacher compression with all the methods and tasks. For *Insert Peg*, we consider two setups, with full and short trajectories in the dataset. See Appendix F

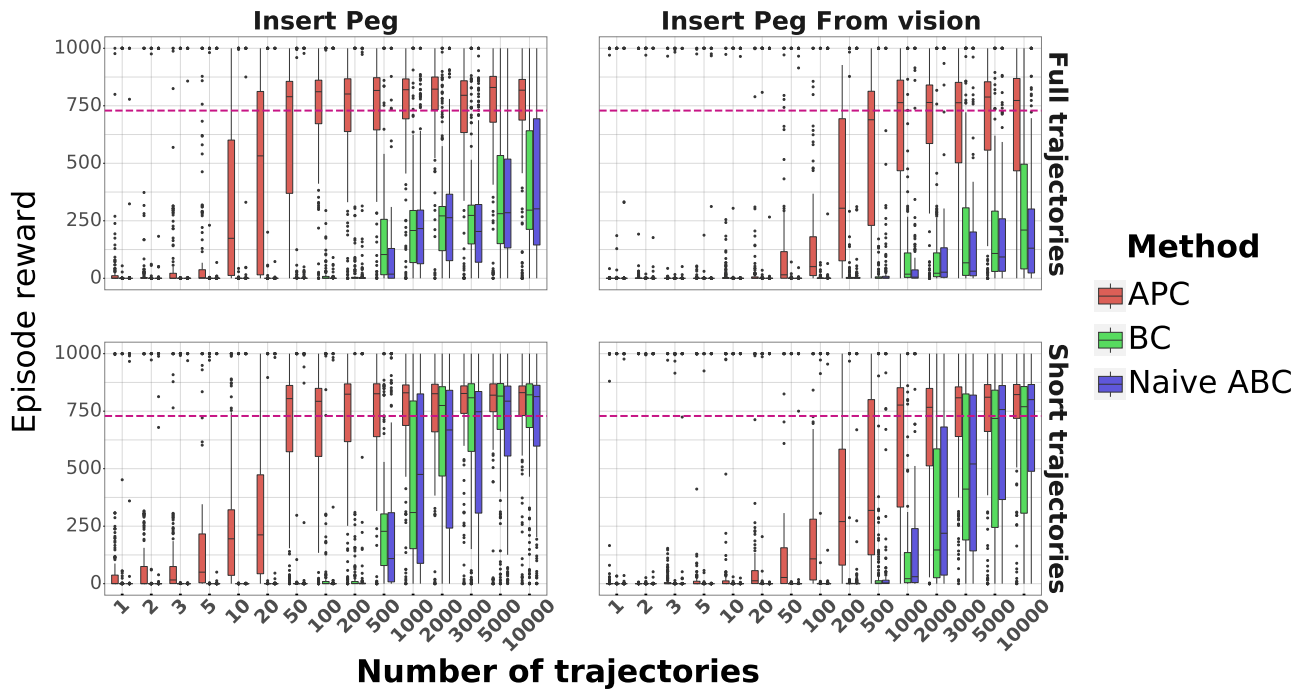


Figure 10. Learning from privileged experts, additional results. On top of the considered results in the main paper, we add additional results with short trajectories.

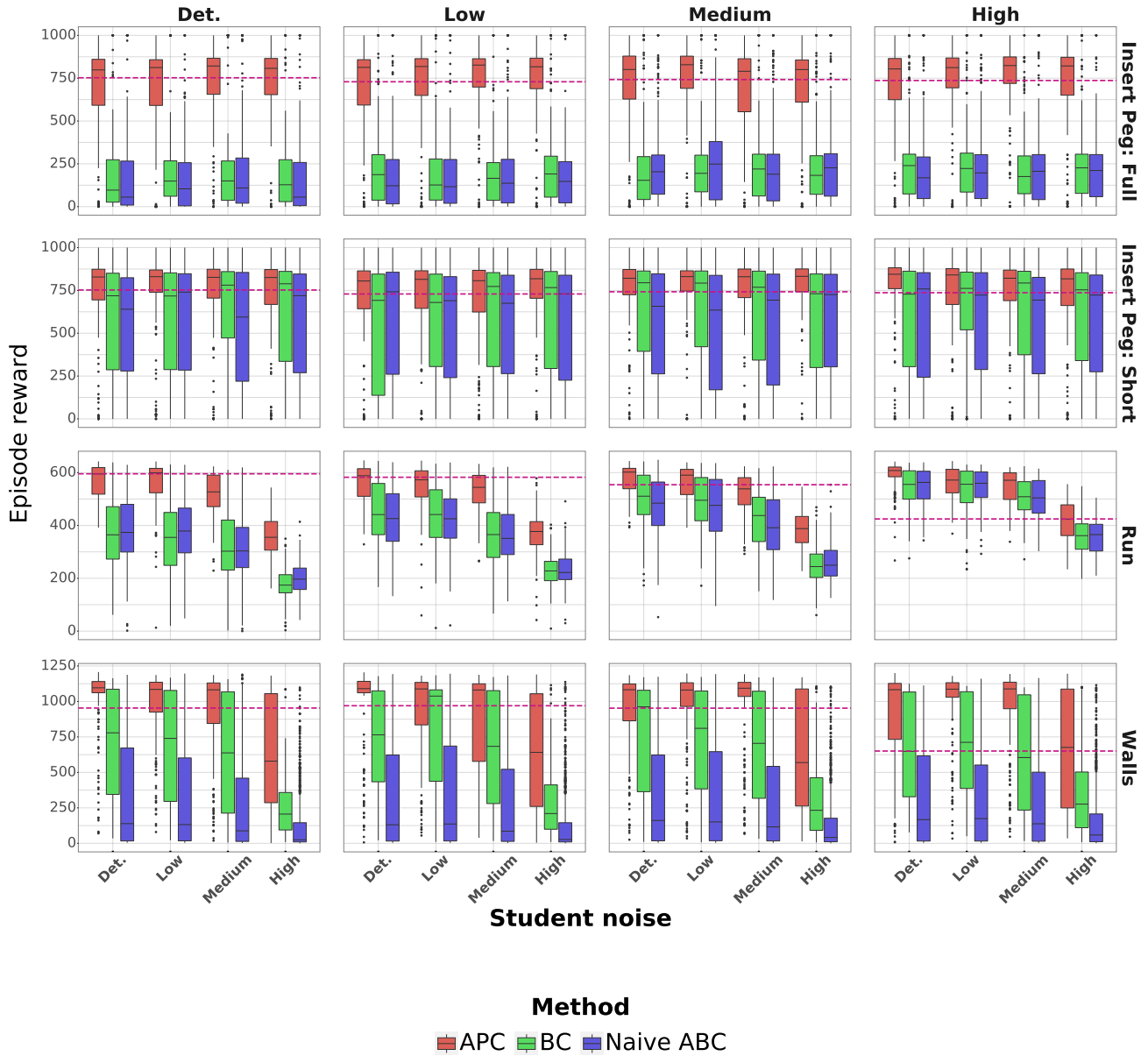


Figure 11. **Noise sensitivity results.** We consider 4 levels of noise for student and expert: **Deterministic**, which uses the Gaussian mean for the action, **Low**, is the noise $\sigma = 0.2$, **Medium** $\sigma = 0.5$ and **High** $\sigma = 1.0$. Each column corresponds to a different level of expert noise. Each row represents different task. For *Insert peg* we consider scenario with full and short trajectories, see Appendix F. For *Humanoid Run* and *Humanoid Walls* tasks, we use 100 trajectories dataset, whereas for *Insert Peg*, we use dataset with 2000 trajectories, as this task is much less data efficient than others. X-axis corresponds to a different level of student noise. Y-axis corresponds to the episodic reward with 150 independent evaluations. The legend denotes a method and a row corresponds to a task. The pink dashed line indicate average expert performance.

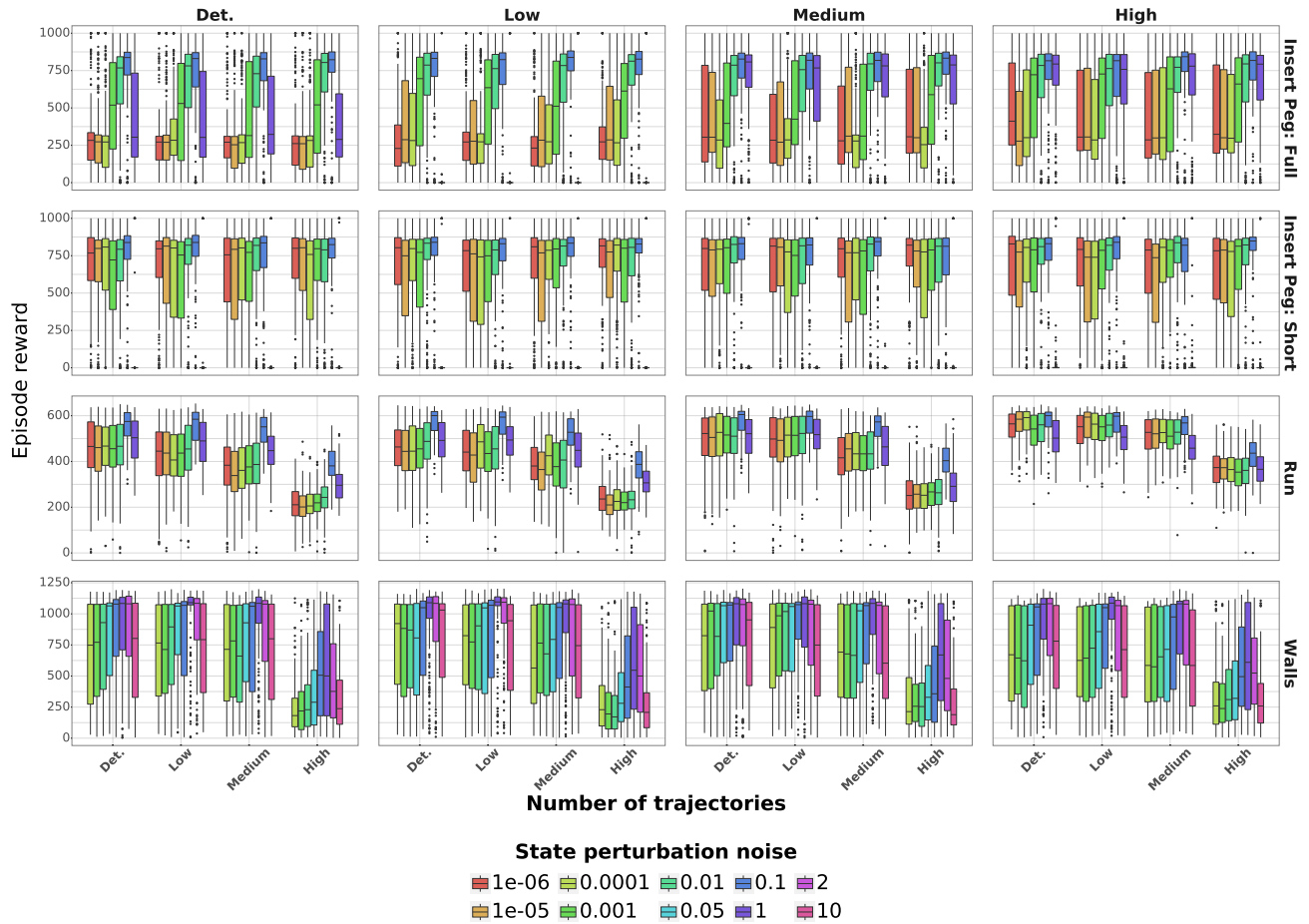


Figure 12. State perturbation noise sensitivity for APC. In this plot we represent the APC method trained on 100 full trajectories sampled under different level of expert noise which is represented by different columns. On the X-axis is the different level of a student noise at evaluation time. The legend denotes different levels of a state perturbation noise σ_s from the eqn. (7) from the main paper. Y-axis corresponds to the episodic reward with 150 independent evaluations.

Data augmentation for efficient learning from parametric experts

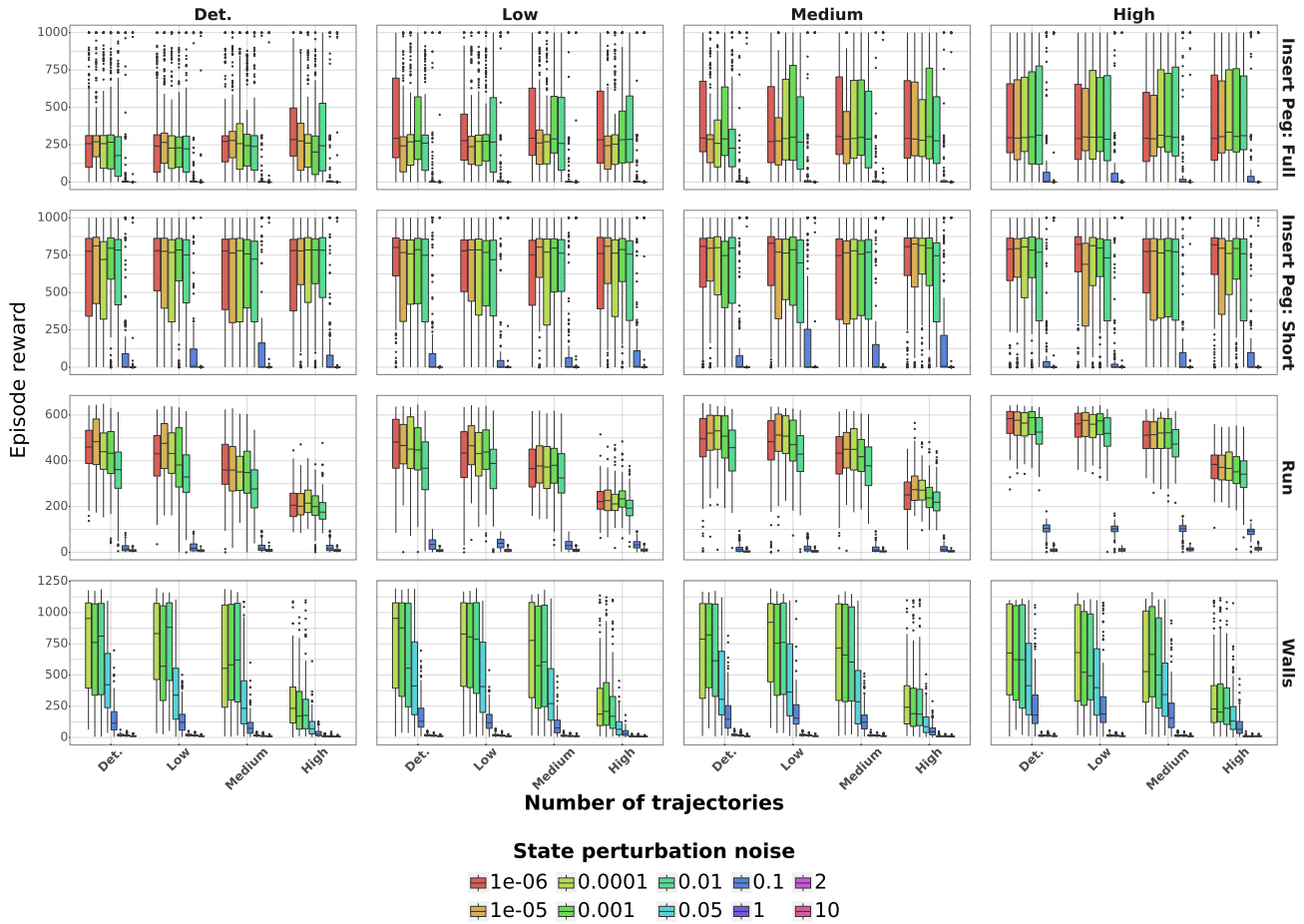


Figure 13. State perturbation noise sensitivity for Naive ABC. In this plot we represent the Naive ABC method trained on 100 full trajectories sampled under different level of expert noise which is represented by different columns. On the X-axis is the different level of a student noise at evaluation time. The legend denotes different levels of a state perturbation noise σ_s from the eqn. (7) from the main paper. Y-axis corresponds to the episodic reward with 150 independent evaluations.

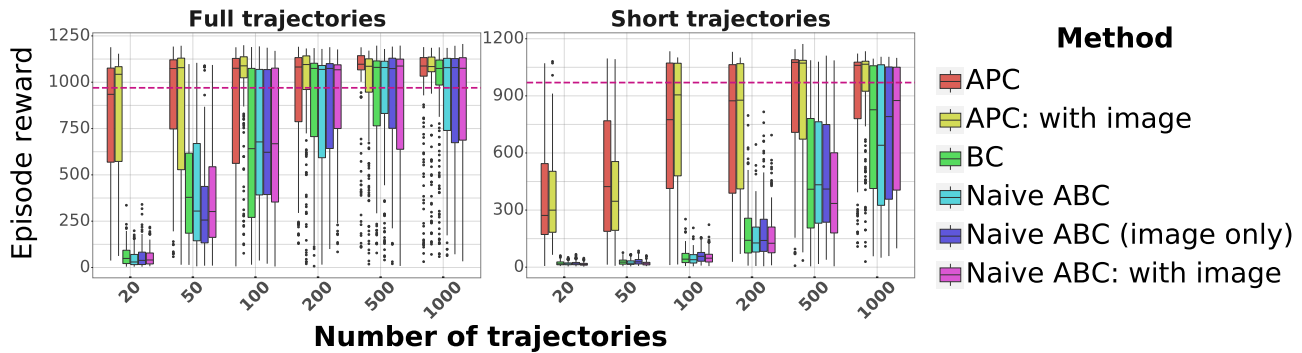


Figure 14. Additional behavioral cloning results on Walls tasks with additional methods added. X-axis corresponds to a number of trajectories used in each of the dataset. The Y-axis corresponds to the episodic reward with 150 random evaluations. The pink dashed line indicate average (among the same 150 independent evaluations) expert performance. The legend describes a method which is used. The plot on the left depicts the performance of offline policy cloning with using full trajectories from the expert, whereas the plot on the right represents the experiment with short trajectories. See Appendix F for more details.

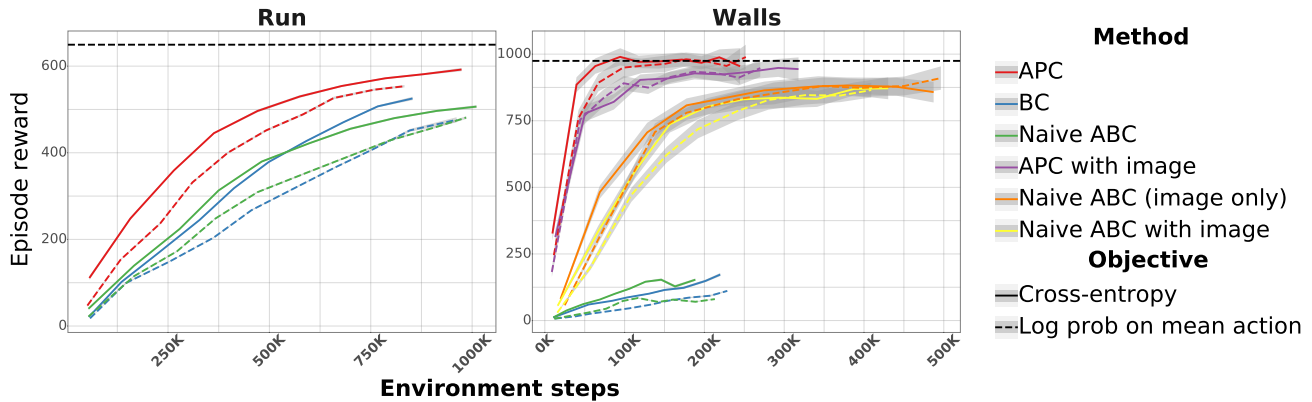


Figure 15. **DAGGER objective sweep with $\beta = 0.0$.** On the X-axis we report the number of environment steps. On the Y-axis we report averaged across 3 seeds episodic reward achieved by the student. Shaded area corresponds to confidence intervals. For a Run task, the confidence intervals are small, so they are not visible. In solid line we report the performance when training using the cross-entropy. In dashed line, we report the performance when training using log probability on the mean action from the expert. All the methods use mean action during evaluation. The black dashed line indicate average (among the same 150 independent evaluations) expert performance for the given expert noise level.

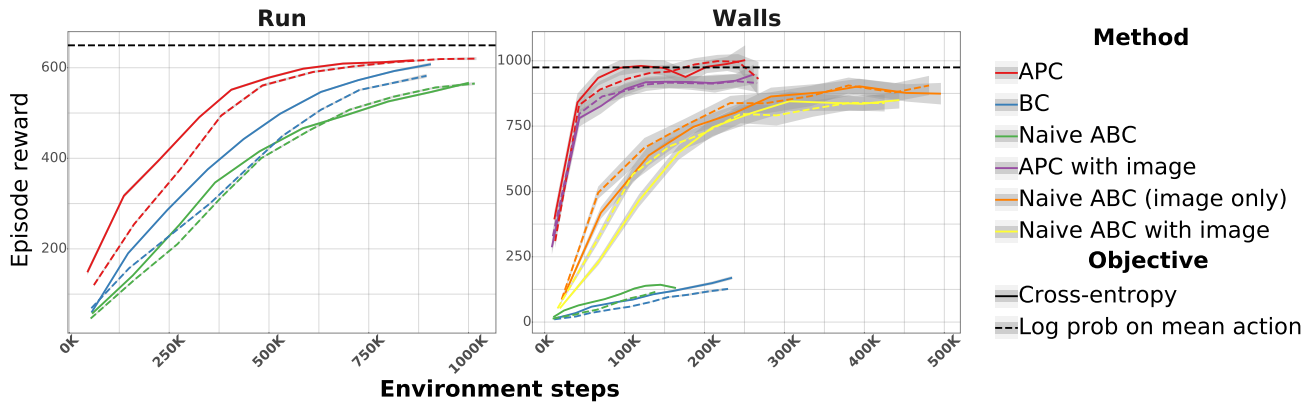


Figure 16. **DAGGER objective sweep with $\beta = 0.3$.** On the X-axis we report the number of environment steps. On the Y-axis we report averaged across 3 seeds episodic reward achieved by the student. Shaded area corresponds to confidence intervals. For a Run task, the confidence intervals are small, so they are not visible. In solid line we report the performance when training using the cross-entropy. In dashed line, we report the performance when training using log probability on the mean action from the expert. All the methods use mean action during evaluation. The black dashed line indicate average (among the same 150 independent evaluations) expert performance for the given expert noise level.